Tuning of a MEMS RF Filter

Bashar K Hammad†, Eihab M Abdel-Rahman‡, and Ali H Nayfeh†

†Dept. of Engineering Science and Mechanics, MC 0219, Virginia Tech,
Blacksburg, Virginia 24061, USA, anayfeh@vt.edu
‡Dept. of Systems Design Engineering, University of Waterloo, Waterloo, ON N2L 3G1, Canada

ABSTRACT

We present an *analytical* model and closed-form expressions describing the response of a tunable MEMS RF filter. It extends our earlier model to general operating conditions by allowing for a combined DC and AC input signal and an independent DC voltage V_{DC2} applied to the output beam. The model is obtained by discretizing the distributed-parameter system using a Galerkin procedure to produce a reduced-order model of the filter. It consists of two nonlinearly coupled ordinary-differential equations of motions. The mismatch in the effective DC voltage applied to the input and output beams modifies the global modes significantly, reflecting localization of the response in either of the two beams. We present results describing variation of the center frequency, bandwidth, and sensitivity with V_{DC2}.

Keywords: MEMS, RF filter, tuning, localization.

1 INTRODUCTION

In modern communication systems, there is a continuous trend towards miniaturization to allow for the integration of transmitters and receivers on the same chip. To ensure that they do not interfere with each other, narrow-band filtering is required. The successful implementation of high-Q micromechanical resonators in many on-chip systems suggests a method for miniaturizing and integrating highly selective filters alongside other IC components. A mechanical filter is composed of two or more mechanically coupled resonators. Bannon et al. [1] first demonstrated filters comprised of two clamped-clamped beams coupled mechanically by a soft spring (a flexural-mode beam) and later presented [2] a step-by-step design procedure for these filters.

A two-resonator filter is made up of two similar resonators and a coupling spring. It has two distinct mode shapes defining the filter bandwidth. In the mode shape associated with the lower end of the bandwidth, the two resonators vibrate in-phase, whereas at the high end of the bandwidth, they vibrate 180° out-of-phase. The bandwidth is determined by the stiffness of the coupling spring, while the center frequency is determined by the frequency of the resonators. Electromechanical filters use an electrode underneath the input resonator to transform the electric signal into an electrostatic force, which is used to vibrate the resonator. The resonator produces measurable motions in the neighborhood of its resonance frequencies only; that is, when the signal frequency is within the bandwidth of the filter. This motion is transmitted to the output resonator via the coupling spring. The output resonator converts the resulting motion into an electrical capacitance sensed by an output electrode.

2 PROBLEM FORMULATION

We consider a filter, Figure 1, composed of two identical clamped-clamped (primary) microbeams of rectangular cross sections connected at their midspans by a weak microbeam. Two electrodes of identical dimensions to the primary beams are patterned underneath them. The input resonator transforms an input signal, $v_1(t) = V_{DC1} + V_{AC}\cos\Omega t$, to an electrostatic force, which actuates the microbeam. A DC voltage V_{DC2} is applied to the output resonator to magnify the RF signal, tune the filter, reduce the insertion loss, and generate an AC current out of the motions of the microbeam. The nondimensional Lagrangian describing the motions of this filter can be written as [3], [4]

$$\mathcal{L} = \sum_{k=1}^{2}\int_0^1 \dot{w}_k^2 dx + T_c^2\int_0^c \dot{w}_c^2 dx - \sum_{k=1}^{2}\int_0^1 (w_k'')^2 dx$$
$$-R_c\int_0^c (w_c'')^2 dx - \sum_{k=1}^{2} P_{p,k}\int_0^1 (w_k')^2 dx - P_c\int_0^c (w_c')^2 dx$$
$$-\frac{\alpha_1}{2}\sum_{k=1}^{2}\left(\int_0^1 (w_k')^2 dx\right)^2 + 2\alpha_2\sum_{k=1}^{2} v_k^2(t)\int_0^1 \frac{1}{1-w_k} \quad (1)$$

where x is the position along each beam's axis, $w(x,t)$ is the downward transverse deflection of the beam, ℓ is the length of the primary beams, and c is the ratio of the length of the coupling beam to ℓ. Throughout this paper, $k = 1$ and $k = 2$ refer to quantities related to the input and output beams, respectively. The parameters

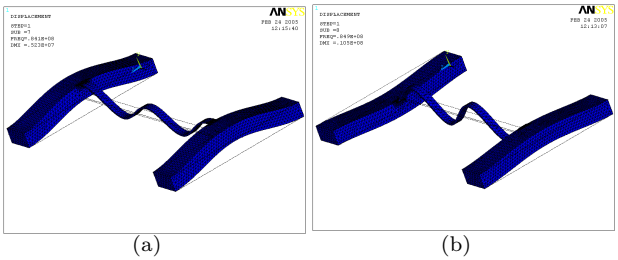

(a) (b)

Figure 1: First (in-phase) (a) and second (out-of-phase) (b) modes of the un-actuated filter.

appearing in equation (1) are

$$T_c^2 = \frac{A_c}{A_p}, \quad R_c = \frac{I_c}{I_p}, \quad P_c = \frac{N_c \ell^2}{E I_p},$$
$$P_{p,k} = \frac{N_{p,k} \ell^2}{E I_p}, \quad \alpha_1 = 6 \left(\frac{d}{h_p} \right)^2, \quad \alpha_2 = \frac{6 \epsilon \ell^4}{E h_p^3 d^3}, \quad (2)$$

where A_p and I_p are the area and moment of inertia of the cross section of the primary beams, A_c and I_c are the area and moment of inertia of the cross section of the coupling beam, $N_{p,k}$ and N_c are the applied tensile axial forces in the primary and coupling beams, b_p is the width of the primary beams, E is Young's modulus, ρ is the material density, d is the gap width, ϵ is the dielectric constant of the capacitor gap medium, and h_p is the primary beams thickness.

Exciting the input beam with a signal near its primary resonance $\Omega \approx \omega_1$, we can approximate the beams response as [5]

$$w_k(x,t) \approx \xi_1(t)\phi_{1,k}(x) + \xi_2(t)\phi_{2,k}(x), \quad k = 1,2,3 \quad (3)$$

where the $\phi_{i,k}$ are the components of the first ϕ_1 and second ϕ_2 global mode shapes of the un-actuated filter on the primary beams $k = 1,2$ and the coupling beam $k = 3$.

Substituting equations (3) into equation (1), writing the Euler-Lagrange equations, and adding damping terms, we obtain the following equations of motion that govern the transverse deflection of the filter:

$$\begin{aligned}
\ddot{\xi}_i \; &+\omega_i^2 \xi_i = -\mu_i \dot{\xi}_i + 2\alpha_2 \Gamma_{1,i} V_{DC1} V_{AC} \cos \Omega t \\
&+\alpha_2 \sum_{k=1}^{2} V_{DCk}^2 \left[\Gamma_{k,i} + 2\Gamma_{k,ii}\, \xi_1 \; + 2\Gamma_{k,ij} \xi_j \right. \\
&+3\Gamma_{k,iii}\, \xi_i^2 + 6\Gamma_{k,iij}\, \xi_i \xi_j + 3\Gamma_{k,ijj}\, \xi_j^2 + 4\Gamma_{k,iiii}\, \xi_i^3 \\
&\left. +12\Gamma_{k,iiij}\, \xi_i^2 \xi_j + 12\Gamma_{k,iijj} \xi_i \xi_j^2 + 4\Gamma_{k,ijjj}\, \xi_j^3 \right] \\
&-\alpha_1 \left[\left(\sum_{k=1}^{2} \Lambda_{k,ii}^2 \right) \xi_i^3 + \left(\sum_{k=1}^{2} \Lambda_{k,ii} \Lambda_{k,jj} \right) \xi_i \xi_j^2 \right. \\
&\left. +2 \left(\sum_{k=1}^{2} \Lambda_{k,ij}^2 \right) \xi_i \xi_j^2 \right], \quad i,j = 1,2 \; (i \neq j) \qquad (4)
\end{aligned}$$

where μ_i is the linear damping coefficient of the i^{th} mode and the coefficients Γ and Λ are functions of the mode shapes.

We decompose the generalized coordinates ξ_i into static $\xi_{s,i}$ and dynamic $\xi_{d,i}(t)$ components: $\xi_i(t) = \xi_{s,i} + \xi_{d,i}(t)$. The $\xi_{s,i}$ are solutions of equations (4) with keeping the time derivatives and the harmonic forcing terms equal to zero. Substituting $\xi_i(t) = \xi_{s,i} + \xi_{d,i}(t)$ into equations (4) and eliminating the terms representing the static equilibrium, we obtain the following equations motion around $\xi_{s,i}$:

$$\begin{aligned}
\ddot{\xi}_{d,i} \; &+\omega_i^2 \xi_{d,i} = -\mu_i \dot{\xi}_{d,i} + 2\alpha_2 \Gamma_{1,i} V_{DC1} V_{AC} \cos \Omega t \\
&+\alpha_2 \sum_{k=1}^{2} V_{DCk}^2 [2\Gamma_{k,ii}\, \xi_{d,i} + 2\Gamma_{k,ij}\, \xi_{d,j} + 3\Gamma_{k,iii} \\
&(\xi_{d,i}^2 + 2\xi_{s,i}\xi_{d,i}) + 6\Gamma_{k,iij} (\xi_{d,i}\xi_{s,j} + \xi_{d,i}\xi_{d,j} + \xi_{d,j}\xi_{s,i}) \\
&+3\Gamma_{k,ijj} (\xi_{d,i}^2 + 2\xi_{s,j}\xi_{d,j}) + 4\Gamma_{k,iiii} (\xi_{d,i}^3 + 3\xi_{s,i}^2 x i_{d,i} \\
&+3\xi_{s,i}\xi_{d,i}^2) + 12\Gamma_{k,iiij} (\xi_{d,i}^2 \xi_{s,j} + 2\xi_{s,i}\xi_{s,j}\xi_{d,i} + \xi_{s,i}^2 \xi_{d,j} \\
&+\xi_{d,i}^2 \xi_{d,j} + 2\xi_{s,i}\xi_{d,i}\xi_{d,j}) + 12\Gamma_{k,iijj} (\xi_{d,j}^2 \xi_{s,i} + 2\xi_{s,i}\xi_{s,j} \\
&\xi_{d,j} + \xi_{s,j}^2 \xi_{d,i} + \xi_{d,j}^2 \xi_{d,i} + 2\xi_{s,j}\xi_{d,i}\xi_{d,j}) + 4\Gamma_{k,ijjj} (\xi_{d,j}^3 \\
&+3\xi_{s,j}^2 \xi_{d,j} + 3\xi_{s,j}\xi_{d,j}^2)] - \alpha_1 [(\sum_{k=1}^{2} \Lambda_{k,ii}^2) (\xi_{d,i}^3 + 3\xi_{s,i}^2 \\
&\xi_{d,i} + 3\xi_{s,i}\xi_{d,i}^2) + (\sum_{k=1}^{2} \Lambda_{k,ii}\Lambda_{k,jj} + 2\sum_{k=1}^{2} \Lambda_{k,ij}^2) \\
&(\xi_{d,j}^2 \xi_{s,i} + 2\xi_{s,i}\xi_{s,j}\xi_{d,j} + \xi_{s,j}^2 \xi_{d,i} + \xi_{d,j}^2 \xi_{d,i} \\
&+2\xi_{s,j}\xi_{d,i}\xi_{d,j})], \qquad i,j = 1,2 \; (i \neq j) \qquad (5)
\end{aligned}$$

3 PERTURBATION ANALYSIS

The filter, by design, has a one-to-one internal resonance between the first two global modes. Hence, for the case of primary resonance of the first mode, we write

$$\omega_2 = \omega_1 + \epsilon^2 \sigma_1 \quad \text{and} \quad \Omega = \omega_1 + \epsilon^2 \sigma_2 \qquad (6)$$

where σ_1 and σ_2 are small detuning parameters and ϵ is a small nondimensional book-keeping parameter. Using the method of multiple scales [6], we seek a first-order uniform approximation to the solution of equations (5) in the form

$$\begin{aligned}
\xi_{d,i} = \xi_{d,i1}(T_o, T_2) &+\epsilon^2 \xi_{d,i2}(T_o, T_2) + \epsilon^3 \xi_{d,i3}(T_o, T_2) \\
&+ \cdots \qquad i = 1,2 \qquad (7)
\end{aligned}$$

where $T_o = t$ and $T_2 = \epsilon^2 t$. Substituting equations (7) into equations (5), using equations (6), and equating coefficients of like powers of ϵ, we obtain the following hierarchy of problems:

Order ϵ

$$\mathcal{L}_1(\xi_{d,11}) = 0 \qquad (8)$$
$$\mathcal{L}_2(\xi_{d,21}) = 0 \qquad (9)$$

Order ϵ^2

$$\mathcal{L}_1(\xi_{d,12}) = \kappa_5 \xi_{d,11}^2 + \kappa_6 \xi_{d,21}^2 + \kappa_7 \xi_{d,11}\xi_{d,21} \qquad (10)$$
$$\mathcal{L}_2(\xi_{d,22}) = \kappa_8 \xi_{d,11}^2 + \kappa_9 \xi_{d,21}^2 + \kappa_{10} \xi_{d,11}\xi_{d,21} \qquad (11)$$

Order ϵ^3

$$\mathcal{L}_1(\xi_{d,13}) = \mathcal{F}_1 \qquad (12)$$
$$\mathcal{L}_2(\xi_{d,23}) = \mathcal{F}_2 \qquad (13)$$

The linear operators can be written as

$$\mathcal{L}_1(\xi_{d,1n}) = D_o^2\xi_{d,1n} + (\omega_1^2 - \kappa_1)\xi_{d,1n} - \kappa_2\xi_{d,2n} \quad (14)$$
$$\mathcal{L}_2(\xi_{d,2n}) = D_o^2\xi_{d,2n} + (\omega_2^2 - \kappa_4)\xi_{d,2n} - \kappa_3\xi_{d,1n} \quad (15)$$

where $n = 1, 2, 3$ and $D_n \equiv \partial/\partial T_n$. The terms $\mathcal{F}_1$ and $\mathcal{F}_2$ in equations (12) and (13) are

$$\begin{aligned}\mathcal{F}_1 = &-2D_oD_2\xi_{d,11} - \mu_1 D_o\xi_{d,11} + \kappa_{11}\xi_{d,11}^3 + \kappa_{12}\xi_{d,21}^3\\ &+\kappa_{13}\xi_{d,11}\xi_{d,21} + \kappa_{14}\xi_{d,11}\xi_{d,22} + \kappa_{15}\xi_{d,12}\xi_{d,21}\\ &+\kappa_{16}\xi_{d,21}\xi_{d,22} + \kappa_{17}\xi_{d,11}^2\xi_{d,21} + \kappa_{18}\xi_{d,11}\xi_{d,21}^2\\ &+2\alpha_2\Gamma_{1,1}V_{DC1}V_{AC}\cos(\lambda_1 T_o + \sigma_2 T_2) \quad (16)\\ \mathcal{F}_2 = &-2D_oD_2\xi_{d,21} - \mu_2 D_o\xi_{d,21} + \kappa_{19}\xi_{d,11}^3 + \kappa_{20}\xi_{d,21}^3\\ &+\kappa_{21}\xi_{d,11}\xi_{d,21} + \kappa_{22}\xi_{d,11}\xi_{d,22} + \kappa_{23}\xi_{d,12}\xi_{d,21} +\\ &+\kappa_{24}\xi_{d,21}\xi_{d,22} + \kappa_{25}\xi_{d,11}^2\xi_{d,21} + \kappa_{26}\xi_{d,11}\xi_{d,21}^2\\ &+2\alpha_2\Gamma_{1,2}V_{DC1}V_{AC}\cos(\lambda_1 T_o + \sigma_2 T_2) \quad (17)\end{aligned}$$

where the coefficients κ_1 to κ_{26} are functions of $\alpha_i, \phi_i, \xi_{s,i}$, and V_{DC1}.

We solve equations (8) to (13) sequentially. The first-order problem, equations (8) and (9), are an eigenvalue problem. Its solution can be expressed as

$$\xi_{d,j1} = A_1(T_2)\, u_{1j}\, e^{i\lambda_1 T_0} + A_2(T_2)\, u_{2j}\, e^{i\lambda_2 T_0} + \text{cc},\ j = 1, 2 \quad (18)$$

where *cc* stands for the complex conjugate of the preceding terms, λ_1 and λ_2 are the eigenvalues (the natural frequencies modified by V_{DC1} and V_{DC2}), and $\mathbf{u_1} = [u_{11} \quad u_{12}]^T$ and $\mathbf{u_2} = [u_{21} \quad u_{22}]^T$ are the eigenvectors. We substitute equations (18) into equations (10) and (11) and solve for $\xi_{d,12}$ and $\xi_{d,22}$. Next, we transform the third-order system (12) and (13) into the modal coordinates of the first-order system (8) and (9). After some manipulation, the third-order equations become:

$$\ddot{\eta}_i + \lambda_i^2\eta_i = u_{i1}\,\mathcal{F}_1 + u_{i2}\,\mathcal{F}_2, \qquad i = 1, 2 \quad (19)$$

Substituting equations (18) and the results for $\xi_{d,12}$ and $\xi_{d,22}$ into equations(19) and eliminating the terms that produce secular terms, we obtain

$$\begin{aligned}&-i\chi_1\lambda_1\dot{A}_1 - i\chi_2\,\lambda_1 A_1 + \chi_3 A_1^2\bar{A}_1 + \chi_4 A_1^2\bar{A}_2 e^{-i\sigma_1 T_2}\\ &+\chi_5\bar{A}_1 A_2^2 e^{2i\sigma_1 T_2} + (\chi_6 A_2^2\bar{A}_2 + \chi_7 A_1\bar{A}_1 A_2)e^{i\sigma_1 T_2}\\ &+\chi_8 A_1 A_2\bar{A}_2 + \alpha_2\chi_9 V_{DC1}V_{AC}e^{i\sigma_2 T_2} = 0 \quad (20)\\ &-i\chi_{10}\lambda_2\dot{A}_2 - i\chi_{11}\,\lambda_2 A_2 + \chi_{12}A_2^2\bar{A}_2 + \chi_{13}A_2^2\bar{A}_1 e^{i\sigma_1 T_2}\\ &+\chi_{14}\bar{A}_2 A_1^2 e^{-2i\sigma_1 T_2} + (\chi_{15}A_1^2\bar{A}_1 + \chi_{16}A_2\bar{A}_2 A_1)e^{-i\sigma_1 T_2}\\ &+\chi_{17}A_1 A_2\bar{A}_1 + \alpha_2\chi_{18}V_{DC1}V_{AC}e^{i(\sigma_2-\sigma_1)T_2} = 0 \quad (21)\end{aligned}$$

where $\chi_1, \chi_2, \cdots, \chi_{18}$ are functions of $\mathbf{u_1}, \mathbf{u_2}$, and κ_1 to κ_{26}.

Introducing the polar form $A_j = \frac{1}{2}a_j e^{i\beta_j}$ into equations (20) and (21), separating real and imaginary parts, and defining the new phase parameters

$$\gamma_1 = -\beta_1 + \beta_2 + \sigma_1 T_2 \ \text{ and } \ \gamma_2 = -\beta_1 + \sigma_2 T_2 \quad (22)$$

we obtain the modulation equations

$$\begin{aligned}\dot{a}_1 = &-\frac{1}{2}\frac{\chi_2}{\chi_1}a_1 - \frac{1}{8}\frac{\chi_4}{\lambda_1\chi_1}a_1^2 a_2\sin\gamma_1 + \frac{1}{8}\frac{\chi_5}{\lambda_1\chi_1}a_1 a_2^2\sin 2\gamma_1\\ &+\frac{1}{8}\frac{\chi_6}{\lambda_1\chi_1}a_2^3\sin\gamma_1 + \frac{1}{8}\frac{\chi_7}{\lambda_1\chi_1}a_1^2 a_2\sin\gamma_1\\ &+\frac{\chi_9}{\lambda_1\chi_1}\alpha_2 V_{DC1}V_{AC}\sin\gamma_2 \quad (23)\\ a_1\dot{\beta}_1 = &-\frac{1}{8}\frac{\chi_3}{\lambda_1\chi_1}a_1^3 - \frac{1}{8}\frac{\chi_4}{\lambda_1\chi_1}a_1^2 a_2\cos\gamma_1 - \frac{\chi_8}{\lambda_1\chi_1}a_1 a_2^2\\ &-\frac{1}{8}\frac{\chi_5}{\lambda_1\chi_1}a_1 a_2^2\cos 2\gamma_1 - \frac{1}{8}\frac{\chi_6}{\lambda_1\chi_1}a_2^3\cos\gamma_1\\ &-\frac{1}{8}\frac{\chi_7}{\lambda_1\chi_1}a_1^2 a_2\cos\gamma_1 - \frac{\chi_9}{\lambda_1\chi_1}\alpha_2 V_{DC1}V_{AC}\cos\gamma_2 \quad (24)\\ \dot{a}_2 = &-\frac{1}{2}\frac{\chi_{11}}{\chi_{10}}a_2 + \frac{1}{8}\frac{\chi_{13}}{\lambda_2\chi_{10}}a_1 a_2^2\sin\gamma_1 - \frac{1}{8}\frac{\chi_{14}}{\lambda_2\chi_{10}}\cdot\\ &a_1^2 a_2\sin 2\gamma_1 - \frac{1}{8}\frac{\chi_{15}}{\lambda_2\chi_{10}}a_1^3\sin\gamma_1 - \frac{1}{8}\frac{\chi_{16}}{\lambda_2\chi_{10}}\cdot\\ &a_1 a_2^2\sin\gamma_1 + \frac{\chi_{18}}{\lambda_2\chi_{10}}\alpha_2 V_{DC1}V_{AC}\sin(\gamma_2-\gamma_1) \quad (25)\\ a_2\dot{\beta}_2 = &-\frac{1}{8}\frac{\chi_{12}}{\lambda_2\chi_{10}} - \frac{1}{8}\frac{\chi_{13}}{\lambda_2\chi_{10}}a_1 a_2^2\cos\gamma_1 - \frac{\chi_{17}}{\lambda_2\chi_{10}}a_1^2 a_2\\ &-\frac{1}{8}\frac{\chi_{14}}{\lambda_2\chi_{10}}a_1^2 a_2\cos 2\gamma_1 - \frac{1}{8}\frac{\chi_{15}}{\lambda_2\chi_{10}}a_1^3\cos\gamma_1 - \frac{1}{8}\frac{\chi_{16}}{\lambda_2\chi_{10}}\cdot\\ &a_1 a_2^2\cos\gamma_1 - \frac{\chi_{18}}{\lambda_2\chi_{10}}\alpha_2 V_{DC1}V_{AC}\cos(\gamma_2-\gamma_2) \quad (26)\end{aligned}$$

Substitute the polar form into equations (18), we obtain a first-order approximation of the generalized coordinates as

$$\begin{aligned}\xi_i = &\xi_{s,i} + u_{1i}\,a_1\,\cos(\Omega t - \gamma_2)\\ &+u_{2i}\,a_2\,\cos(\Omega t + \gamma_1 - \gamma_2),\ i = 1, 2 \quad (27)\end{aligned}$$

where γ_i are given by equations (22). Substituting equations (27) into equations (3), we obtain the response of the filter, to first approximation, to a primary resonance excitation as

$$\begin{aligned}w_k(x,t) = &\sum\nolimits_{i=1}^{2}[\xi_{s,i} + u_{1i}\,a_1\cos(\Omega t - \gamma_2) \quad (28)\\ &+u_{2i}\,a_2\cos(\Omega t + \gamma_1 - \gamma_2)]\phi_{i,k}(x),\ k = 1, 2\end{aligned}$$

4 RESULTS AND DISCUSSION

For a filter made out of two identical resonators with the specifications listed in [4], we used ANSYS to find the first $\phi_1(x)$ and second $\phi_2(x)$ global modes of the filter shown in Figures 1a and 1b, respectively. The first two natural frequencies of the filter were found to be $\omega_1 = 86.099$ MHz and $\omega_2 = 86.174$ MHz, indicating an initial center frequency of 86.136 MHz when no DC voltage was applied to the filter.

We found that applying a mismatched DC voltage to the input and output beams modifies the global modes significantly. We show in Figure 2 the mode shapes

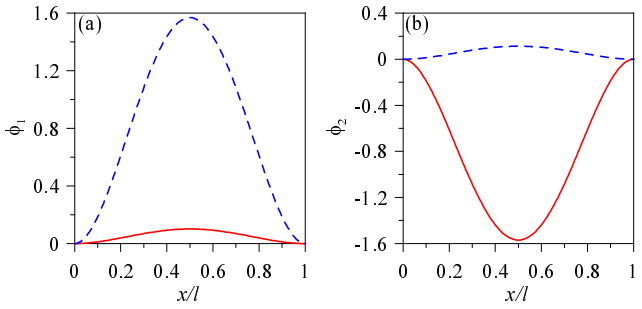

Figure 2: The input beam (solid red lines) and output beam (dashed blue lines) profiles in the first and second global modes when $V_{DC1} = 100V$ and $V_{DC2} = 110V$: (a) First mode and (b) second mode.

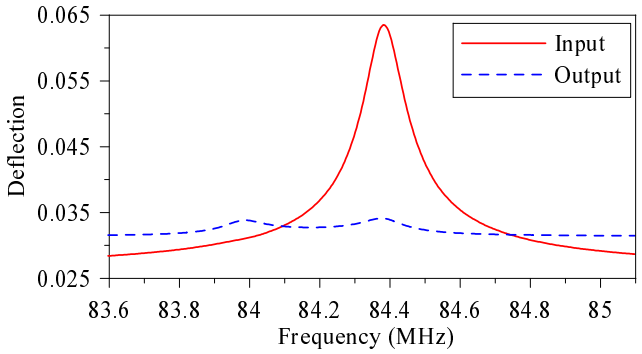

Figure 3: Input beam (solid red line) and output beam (dashed blue line) frequency-response curves when $V_{AC} = 0.1V$.

when $V_{DC1} = 100$V and $V_{DC2} = 110$V. We can identify an input-beam dominant mode and an output-beam dominant mode, reflecting localization of the response in either of the two beams. Due to this localization and for $V_{AC} = 0.1$V, the frequency-response curve of the input beam, Figure 3, exhibits a single peak, while that of the output beam exhibits two closely spaced peaks.

To examine the tunability of the filter, we set $V_{DC1} = 100$V and varied V_{DC2} in the range $90 - 110$V. We obtained a monotonically linear decrease in the center frequency of the filter, Figure 4a, with the increase in V_{DC2} and a monotonically linear broadening of the bandwidth of the filter, Figure 4b, as V_{DC2} is varied away from V_{DC1}.

We examined the impact of these variations in V_{DC2} on the insertion loss by measuring the filter sensitivity, defined as the difference between the maximum deflection of the output beam at the peak (ω_1 or ω_2) and its floor response (away from ω_1 and ω_2), for an input signal of $V_{DC1} = 100$V and $V_{AC}= 0.1$V. Figure 5 shows that the sensitivity decreases (the insertion loss increases) as V_{DC2} moves away from V_{DC1}. So while, V_{DC2} (and/or V_{DC1}) can be used to *tune* the filter, by shifting the center frequency up or down and broadening or contracting

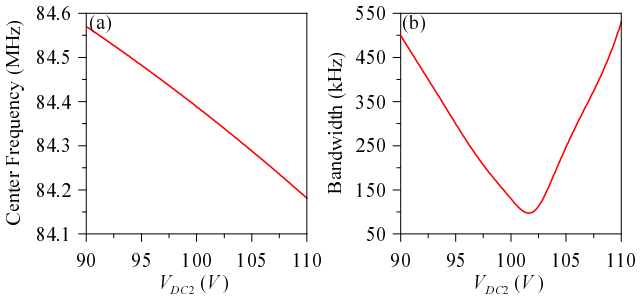

Figure 4: Filter tunability when $V_{DC1} = 100V$: (a) Center frequency and (b) bandwidth.

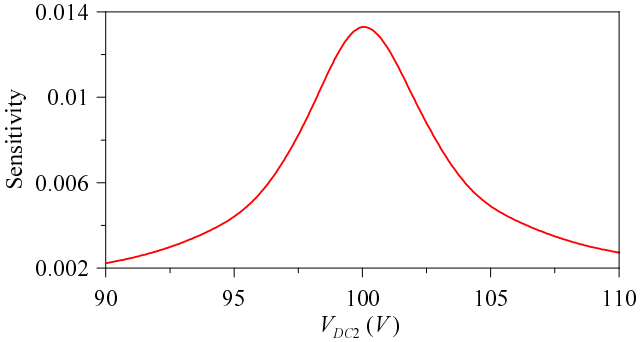

Figure 5: Filter sensitivity when $V_{DC1} = 100V$ and $V_{AC} = 0.1V$.

the bandwidth, this tuning impacts on the insertion loss negatively, thereby limiting the available tuning range.

In conclusion, we derived a compact, analytical approximation for the response of a MEMS RF filter in the form of four first-order ODEs. We solved these equations and used the resulting closed-form expressions to study the filter tunability and insertion loss.

REFERENCES

[1] F. Bannon, J. Clark, and C. Nguyen, "High frequency microelectromechanical IF filter," *Proc. Int. Electon Devices Meeting*, pp. 773–779, 1996.

[2] F. Bannon, J. Clark, and C. Nguyen, "High-Q HF microelectromechanical filters," *J. Solid-State Circuits*, Vol. 35, pp. 512–526, 2000.

[3] A. H. Nayfeh, *Nonlinear Interactions,* Wiley, New York, 2000.

[4] E. M. Abdel-Rahman, B. K. Hammad, and A. H. Nayfeh, "Simulation of a MEMS RF Filter," *Proc of IDETC'05,* DETC2005-85329.

[5] M. I., Younis, E. M. Abdel-Rahman, and A. H. Nayfeh, "A Reduced-order model for electrically actuated microbeam-based MEMS," *J. Microelectromech. Syst.*, Vol. 12, pp. 672–680, 2003.

[6] A. H. Nayfeh, *Introduction to Perturbation Techniques,* Wiley, New York, 1981.